ELSEVIER

Journal of Alloys and Compounds 334 (2002) 304–312

Journal of ALLOYS AND COMPOUNDS

www.elsevier.com/locate/jallcom

Formation of nanocrystalline magnetite by thermal decomposition of iron choline citrate

B. Gržeta[a], M. Ristić[a], I. Nowik[b], S. Musić[a,*]

[a]*Ruđer Bošković Institute, P.O. Box 180, HR-10002 Zagreb, Croatia*
[b]*Racah Institute of Physics, The Hebrew University, IL-91904 Jerusalem, Israel*

Received 9 May 2001; accepted 6 August 2001

Abstract

Thermal decomposition of iron choline citrate ($C_{33}H_{57}Fe_2N_3O_{24}$) has been investigated using X-ray powder diffraction, Fourier transform infrared and ^{57}Fe Mössbauer spectroscopies. The starting compound was heated in a furnace at selected temperatures between room temperature and 460°C, and cooled down afterwards either by quenching in bidistilled water or by cooling in air. Final decomposition products were iron oxides Fe_3O_4 (magnetite) and α-Fe_2O_3 (hematite). In all samples quenched in bidistilled water magnetite was found to be a dominant crystalline phase. Self-propagating burning of iron choline citrate in air was observed. The unit-cell parameter of the obtained magnetite decreased gradually with the increase in temperature of thermal treatment of the starting compound regardless of the cooling procedure. Crystallite size of magnetite varied from 10(1) to 21(2) nm, whereas the crystallite size of hematite varied between 25(2) and 39(3) nm. FT–IR spectra showed a significant amount of organic fraction in the samples containing magnetite as a dominant crystalline phase. In absence (or presence of a small quantity) of organic phase, a transformation of magnetite to hematite occurred. The Mössbauer spectrum of iron choline citrate at RT showed a single line with pronounced broadening. On heating the starting compound at 270°C and quenching in bidistilled water a quadrupole doublet was recorded at RT. This quadrupole doublet was ascribed to amorphous iron(III)-(hydrous) oxide. For samples thermally treated at higher temperatures Mössbauer spectroscopy showed magnetite and hematite. Mössbauer spectra also showed substoichiometric magnetite, $Fe_{3-x}O_4$, which was very pronounced in samples produced at the highest temperatures, and this was in agreement with XRD investigations.

Keywords: Oxide materials; Chemical synthesis; X-ray diffraction; Mössbauer spectroscopy; FT–IR spectroscopy; DTA

1. Introduction

Over the last decade considerable research activities have focused on the synthesis of magnetic oxide particles and their physical and chemical properties. Various magnetic oxide particles have already found important applications (magnetic tapes, magnetic memories, magneto–optical readers, ferrite cores, wave-guides, transformers, etc.). Among magnetic metal oxides, Fe_3O_4 (magnetite) shows unique magnetic and electrical properties. For this reason, magnetite has been the subject of investigations from different standpoints for many decades.

The crystal structure of magnetite was solved by Verwey and de Boer [1] and refined by Fleet [2,3]. Magnetite is a cubic crystal of the spinel series, space group *Fd3m*. The lattice constant of stoichiometric F_3O_4 is a=8.394(5) Å [4]. For a natural magnetite sample Fleet found a= 8.3941(7) Å [2]. There are two distinct Fe sites in the structure: Fe^{3+} ions are at tetrahedral sites, whereas Fe^{2+} and Fe^{3+} ions are equally distributed at octahedral sites of the spinel-type structure. At about ~−153°C magnetite undergoes a sharp phase transition often cited in literature as the Verwey transition, with a characteristic transition temperature T_v. This transition is related to an abrupt decrease in electric conductivity and a specific heat anomaly. At room temperature (RT), ^{57}Fe Mössbauer spectrum of magnetite is characterized with two hyperfine magnetic splitting components. However, in the region of the Verwey transition and at temperatures below it, the Mössbauer spectra are very complicated. Hargrove and Kündig [5] reported that more than two sextets are present in the region of Verwey transition. Later investigations [6–9] confirmed this finding, and several sextets were

*Corresponding author.
E-mail address: music@rudjer.irb.hr (S. Musić).

0925-8388/02/$ – see front matter
PII: S0925-8388(01)01792-3

found; however, there are still uncertainties about their origin. An insight into the origin of these sextets is extremely important for understanding the nature of spontaneous magnetism in magnetite.

Physical and chemical properties of magnetite greatly depend on the route of its synthesis, and for that reason researchers have been using various approaches to the synthesis of magnetite in order to change its properties in a controlled way. Thermal decomposition of Fe-bearing precursors is a very popular way to produce iron oxides, including magnetite. De Abreu Filho et al. [10] reported preparation of magnetite by heating iron(III)-hydroxoacetate above 250°C in a nitrogen atmosphere. Tang et al. [11] used the pyrolysis of aerosol droplets of $Fe_2(SO_4)_3$ solution. Pyrolysis was performed in nitrogen or air atmosphere, and in the samples a mixture of hematite, maghemite and magnetite was detected. The mechanochemical transformation of α-Fe_2O_3 to Fe_3O_4 in vacuum has been monitored by Mössbauer spectroscopy [12]. The magnetite obtained exhibited hyperfine magnetic fields of 459 kOe at tetrahedral Fe sites, and 490 kOe at octahedral Fe sites. Furthermore, Mössbauer spectroscopy was used to monitor the precipitation of magnetite particles from $FeCl_2/2FeCl_3$ solutions containing polyvinyl alcohol at pH~11 [13].

The researchers also focused on the formation of thin magnetite films. For example, Tanaka et al. [14] coated the surface of silica glass with iron(III)-(hydrous)oxide sols. On heating at 940°C a thin α-Fe_2O_3 film was formed and then reduced with carbon to magnetite at 510–630°C in N_2 atmosphere. Thin magnetite films were also epitaxially grown on α-Al_2O_3 and MgO substrates [15], with a better interfacial lattice matching found for the MgO substrate.

Synthesis of magnetic oxides by thermal decomposition of iron–organic compounds has several advantages, such as a relatively low temperature of formation of magnetic oxides, a short reaction time (at times just a few minutes) and a possibility of using inexpensive iron–organic compounds. The properties of the end decomposition product depend on the chemical nature of the precursor used, temperature and reaction atmosphere. In spite of the fact that these reactions are not easy to control, especially the case of a self-propagating burning effect, they are very popular in technology.

In the present work, we have investigated the thermal decomposition of iron choline citrate, $C_{33}H_{57}Fe_2N_3O_{24}$. The phase composition and structural properties of the thermal decomposition products were characterized by X-ray powder diffraction, Fourier transform infrared and ^{57}Fe Mössbauer spectroscopies. Iron choline citrate was found to be suitable for preparation of nanocrystalline magnetite.

2. Experimental

Iron choline citrate (ICC sample) was used as received from SIGMA. The starting chemical was pressed into pellets. The pellets were heated in a tubular furnace in the temperature range between 270 and 460°C, and quenched afterwards in bidistilled water or cooled in air. Experimental conditions for the preparation of the samples and their notation are given in Table 1. The samples AR2, AR3 and AR4 when taken out from the furnace showed a self-propagating burning before being cooled down in air.

Table 1
Experimental conditions for the preparation of samples and their notation

Sample	Temperature of heating (°C)	Period of heating (min)	Mode of cooling
AQ1	270	30	Quenched in bidistilled water
AQ2	350	30	Quenched in bidistilled water
AQ3	425	30	Quenched in bidistilled water
AR1	270	30	Cooled in air
AR2	310	30	Cooled in air
AR3	325	30	Cooled in air
AR4	460	30	Cooled in air

X-ray powder diffraction measurements were performed at RT using a Philips MPD 1880 counter diffractometer, with monochromatized Cu K_α radiation. Diffraction patterns were scanned in steps of 0.02° (2θ) with a fixed counting time of 5 s per step. Two diffraction patterns for each sample were taken (except for the samples AQ1 and AR1), one of a pure sample and the other of a sample admixed with 20% fluorite (CaF_2) to be used as an internal standard. The latter pattern was taken for the purpose of quantitative phase analysis, and for precise determination of unit-cell parameters of crystalline phases.

Fourier transform infrared (FT–IR) spectra of the specimens pressed into KBr discs were recorded at RT using a Perkin-Elmer spectrometer, model 2000. The spectra were processed by means of IR Data Manager (IRDM) program. ^{57}Fe Mössbauer spectra were recorded at RT using conventional nuclear spectroscopic instrumentation. ^{57}Co in a rhodium matrix was used as a Mössbauer source. Isomer shifts were measured relative to α-Fe.

Differential thermal analysis (DTA) was performed for the starting material, iron choline citrate, by means of a Gebrüder Netzsch device. The DTA measurements were made in air and argon atmosphere using a heating rate of 10°C min^{-1}.

3. Results and discussion

3.1. X-ray powder diffraction

Characteristic parts of XRD patterns of the examined samples are shown in Fig. 1 (starting compound and samples quenched in bidistilled water) and Fig. 2 (samples cooled in air). Crystalline phases found in the samples were identified according to data contained in the JCPDS

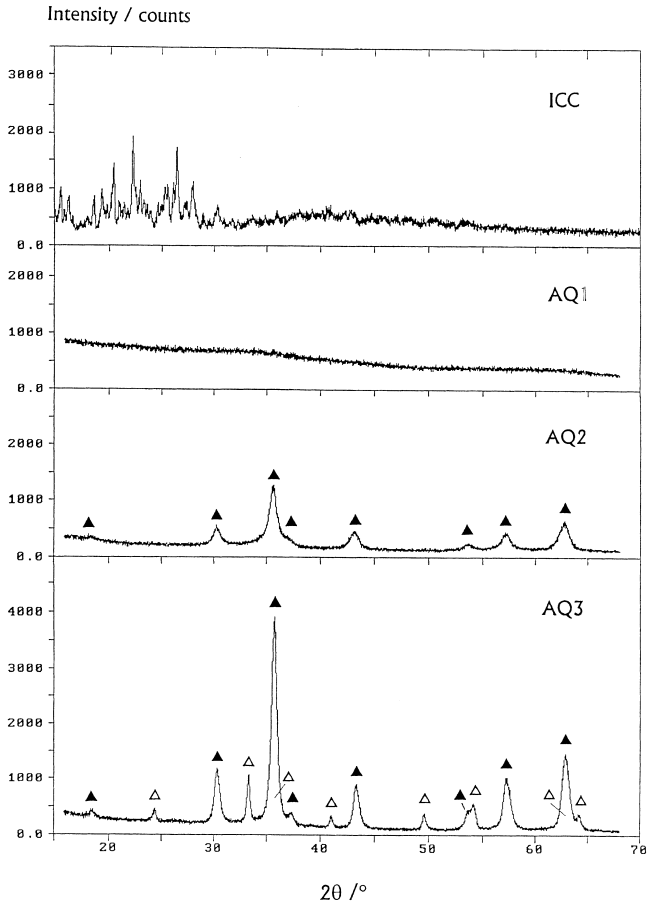

Fig. 1. Characteristic parts of X-ray powder diffraction patterns of iron choline citrate ($C_{33}H_{57}Fe_2N_3O_{24}$) and of samples AQ1, AQ2, AQ3 recorded at RT (▲ Fe_3O_4, △ α-Fe_2O_3).

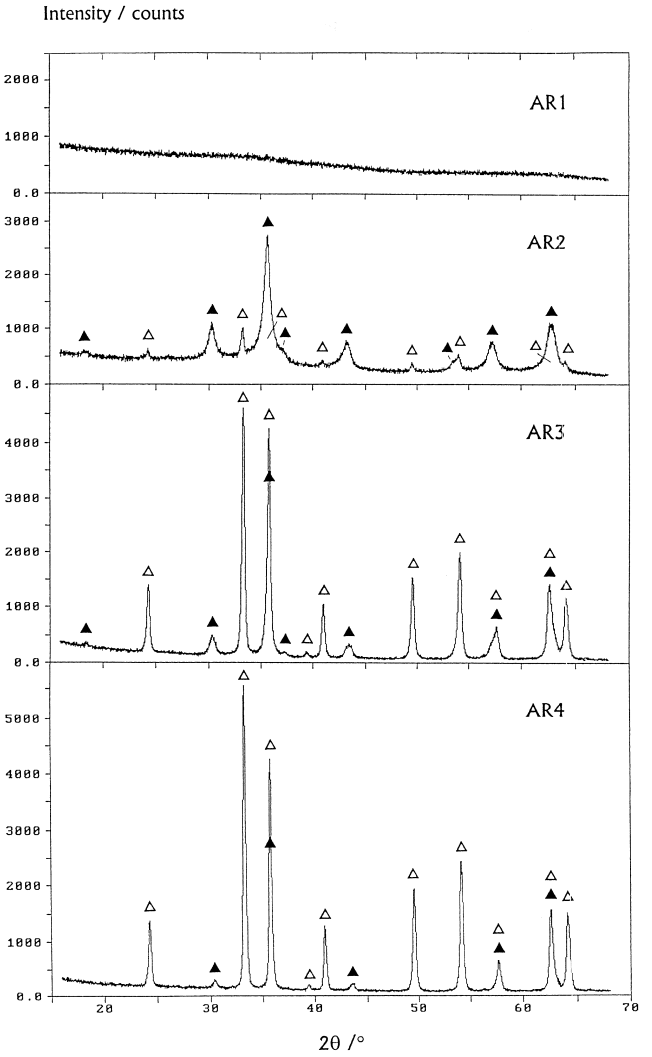

Fig. 2. Characteristic parts of X-ray powder diffraction patterns of samples AR1, AR2, AR3, and AR4, recorded at RT (▲ Fe_3O_4, △ α-Fe_2O_3).

Powder Diffraction File [16]. The results of the XRD phase analysis are given in Table 2. The iron oxide phases magnetite and hematite are the crystalline products of thermal decomposition of the starting compound. The types and fractions of iron oxides formed are dependent on temperature and mode of thermal treatment. The DTA curve in air showed a strong endothermic peak at 245°C due to amorphization of iron choline citrate, whereas in argon a strong endothermic peak was measured at 250°C. The sample heated at 270°C and quenched in bidistilled water (sample AQ1) was completely amorphous, whereas the sample heated at 350°C (sample AQ2) showed diffraction lines characteristic for magnetite and also the presence of an amorphous component. A further increase in temperature caused the appearance of hematite lines in addition to those of magnetite (sample AQ3), with magnetite being the dominant phase. On the other hand, with samples heated at similar temperatures but cooled in air (samples AR2, AR3, AR4), hematite was already well pronounced at 310°C and became the dominant oxide phase at ~325°C, while the fraction of the amorphous component was smaller. Quantitative data were obtained by application of the internal-standard method proposed by Klug and Alexander [17]. Sets of synthetic powder mixtures of magnetite/hematite were prepared and each admixed with 20 wt% of flourite, CaF_2, used as an internal standard. Integrated intensities of diffraction lines 104 of hematite, 220 of magnetite and 111 of flourite for these mixtures were determined using the individual profile fitting [18]. From these intensities the calibration curves for determination of the magnetite and hematite contents were made,

Table 2
Phase composition of samples, determined by X-ray powder diffraction

Sample	Phase composition (weight fraction)[a]
AQ1	Amorphous
AQ2	Amorphous (0.65) + Fe_3O_4 (0.32) + α-Fe_2O_3 (0.03)
AQ3	Amorphous (0.25) + Fe_3O_4 (0.62) + α-Fe_2O_3 (0.13)
AR1	Amorphous
AR2	Amorphous (0.50) + Fe_3O_4 (0.43) + α-Fe_2O_3 (0.07)
AR3	Amorphous (0.15) + Fe_3O_4 (0.20) + α-Fe_2O_3 (0.65)
AR4	Amorphous (0.10) + Fe_3O_4 (0.14) + α-Fe_2O_3 (0.76)

[a] The weight fractions were determined with relative error of 10%.

as shown in Fig. 3. Then the same fraction of flourite was added to the investigated samples and from the integrated intensity ratios of the same diffraction lines of magnetite/hematite and flourite quantitative data were obtained. Selected individual profile fitting results for the purpose of quantitative phase analysis are indicated in Fig. 4.

For all samples diffraction lines of magnetite exhibited a shift to higher Bragg angles compared with JCPDS data, card 19-629 [16]. The effect was more evident as the temperature of thermal treatment increased. This shift of diffraction lines indicated a decrease in the lattice constant of magnetite and possible substoichiometry, $Fe_{3-x}O_4$. Unit-cell parameters of the obtained magnetite and hematite were determined using a method proposed by Toraya [19] by means of the UNITCELL computer program. Angle positions of several diffraction lines of a given iron oxide and three diffraction lines of the internal standard, CaF_2, were determined by individual profile fitting [18] and taken as input data for the program. Obtained unit-cell parameters were refined by the whole-powder-pattern decomposition method using the WPPF program [18]. The fitting of the system sample+CaF_2 was performed in the range $2\theta = 10°–100°$ using the split-type pseudo-Voigt profile function and the polynomial background model. The observed and calculated powder patterns of selected samples are shown in Fig. 5. Whole-powder-pattern fitting showed that sample AQ2 besides magnetite and amorphous phase also contained about 3% hematite. Unit-cell parameters for hematite in all samples agreed with the data given in the JCPDS card 13-534 [16]. The refined unit-cell parameter *a* for magnetite was constantly smaller than reported in literature [2,4,16(card19–629)], as listed in Table 3.

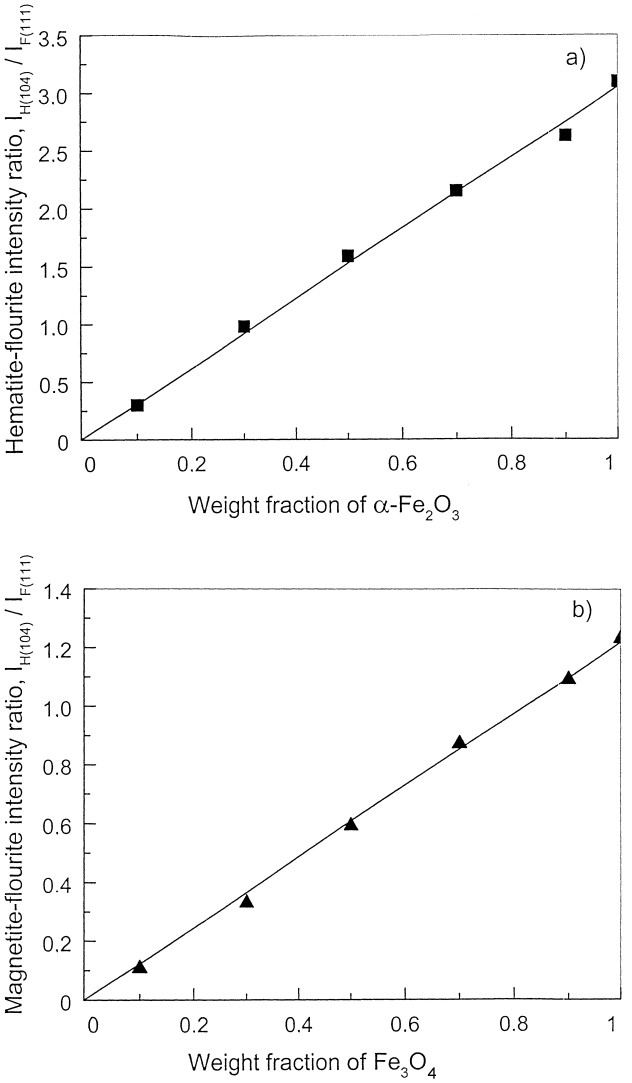

Fig. 3. Calibration curves for determination of weight fractions of (a) hematite and (b) magnetite, using flourite (CaF_2) as internal standard.

Both magnetite and hematite showed diffraction line broadening, which was more pronounced for magnetite, and in both cases decreased with the temperature of thermal treatment, as evident from Figs. 1, 2 and 4. The line broadening was analyzed by the method of line profile widths using a correction curve for diffractometer line profiles as derived by Alexander [20]. Individual profile fitting [18] was used to determine precisely the full widths at half-maximum (FWHM) of the observed diffraction lines of our samples, and also of very pure Si powder used for the instrumental profile correction. The full widths at half-maximum of resulting pure diffraction profiles for both iron oxide phases, Fe_3O_4 and α-Fe_2O_3, increased with the Bragg angle as $1/\cos\theta$, indicating that small crystallite sizes caused line broadening. The crystallite sizes of iron oxide phases were calculated by means of the Scherrer formula, and the values are given in Table 4.

3.2. Fourier transform infrared and Mössbauer spectra

The FT–IR spectrum of iron choline citrate and spectra of samples quenched in water are shown in Fig. 6. The FT–IR spectrum of AQ1 sample shows a very strong and broad band centered at 3402 cm^{-1}. This spectral region corresponds to the stretching vibrations of H_2O. A very strong and broad IR band centered at 480 cm^{-1} is also visible. This IR band usually appears in the presence of amorphous iron(III)-(hydrous)oxide. In the mid-region two very strong IR bands at 1603 and 1400 cm^{-1} with shoulders at 1722 and 1260 cm^{-1} are present. The difference between the asymmetric stretching vibrations $\nu_{as}(COO^-)$ and symmetric stretches $\nu_s(COO^-)$ of 203 cm^{-1} indicates a possibility of the presence of 'free' carboxylate groups in the sample. This means that the basic iron choline citrate structure was destroyed and that the organic intermediate is no more crystalline which is in accordance with X-ray powder diffraction measurements. However, the fraction of this organic intermediate is high enough to reduce Fe^{3+} ions with a further increase in temperature. This is actually confirmed by the FT–IR spectrum of AQ2 sample. Two IR bands located at 580 and 400 cm^{-1} correspond to magnetite. The IR bands of the

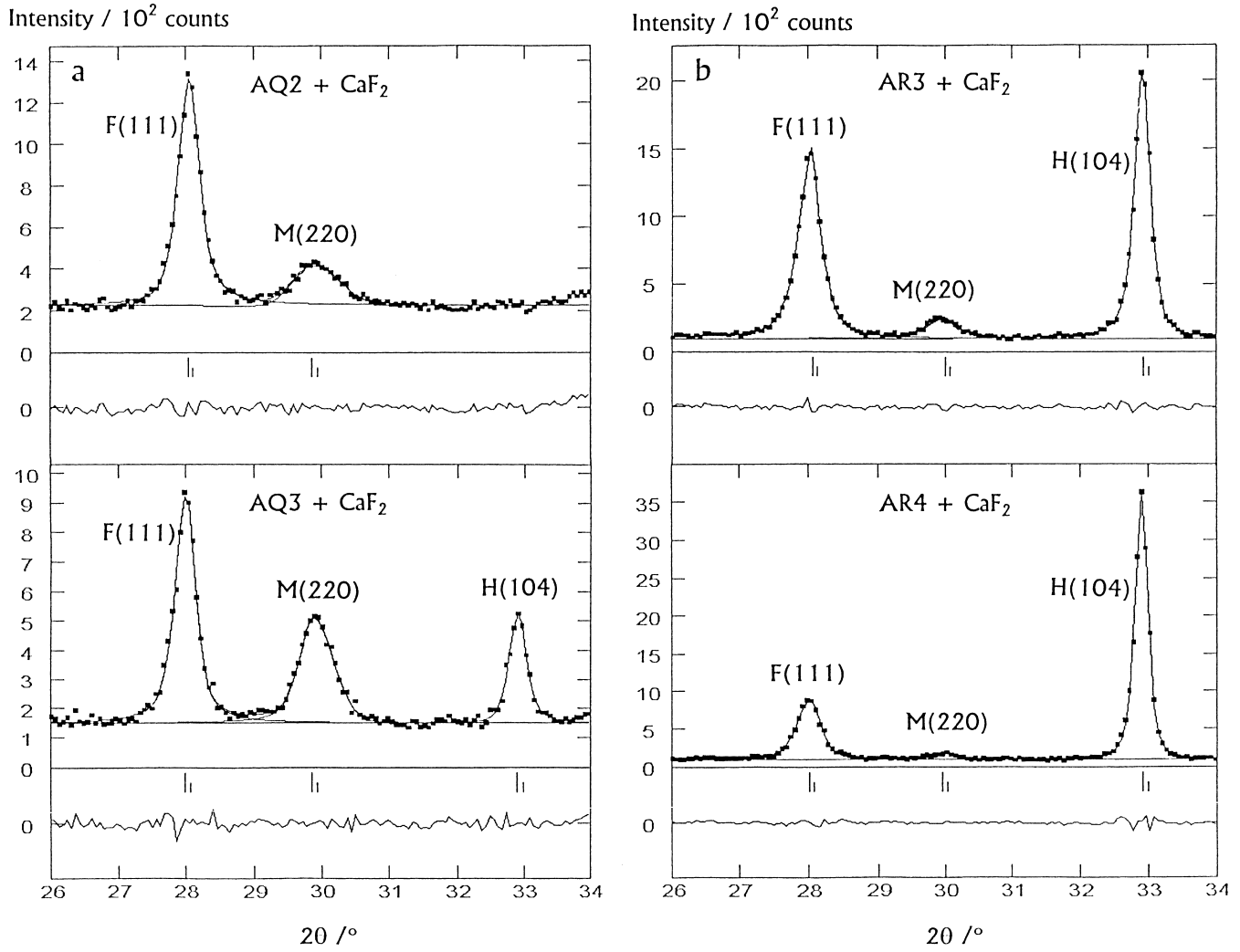

Fig. 4. Individual profile fitting results of selected diffraction lines of magnetite (M), hematite (H) and flourite (F) for the mixtures (a) AQ2+CaF_2 and AQ_3+CaF_2, (b) AR3+CaF_2 and AR3+CaF_2. The split-type pseudo-Voigt profile model was used in calculations.

organic fraction are still present, but decreased in their intensities. FT–IR spectrum of AQ3 sample shows the appearance of an IR band at 441 cm^{-1}, and taking into account the results of XRD measurements this band can be ascribed to hematite. Consequently, there is a shift of IR band from 580 cm^{-1} to 568 cm^{-1}, due to an overlap of the band at 580 cm^{-1} with the second prominent band of hematite. The AQ3 sample contained a much smaller amount of the organic fraction than the AQ2 sample, as can be deduced on the basis of its IR spectrum. From this point of view it is easy to understand why with a further increase in temperature reoxidation of Fe^{2+} occurs. Spectra of samples AR3 and AR4, shown in Fig. 7, exhibited the main features of a hematite spectrum, which is in accordance with the results of the quantitative phase analysis given in Table 2. That is, small organic (amorphous) fraction in these samples, being a consequence of the self-propagating burning before the cooling of samples, favored the formation of hematite. The IR spectrum of hematite and the influence of some factors on this spectrum such as the particle shape, aggregation and matrix, have been discussed by Iglesias et al. [21,22].

Fig. 8 shows the RT Mössbauer spectra of iron choline citrate (ICC sample) and AQ1 sample. The singlet corresponding to iron choline citrate shows a significant broadening and shape typical for a relaxation-type Mössbauer spectrum. On heating the starting compound at 270°C a pure quadrupole interaction is obtained with the parameters $\delta_{Fe}=0.37$ mm s^{-1} and $1/2eqQ=0.84$ mm s^{-1}. These values can be ascribed to an amorphous iron(III)-(hydrous)oxide. Fig. 9 shows the RT Mössbauer spectra of samples AQ2 and AQ3, as well as the spectrum of the magnetite standard for comparison. Mössbauer spectrum of magnetite standard showed full stoichiometry, Fe_3O_4 with the parameters corresponding to the literature data [23]. The AQ2 sample shows superposition of two hyperfine magnetic splitting components and the central quadrupole doublet. These two hyperfine magnetic splitting compo-

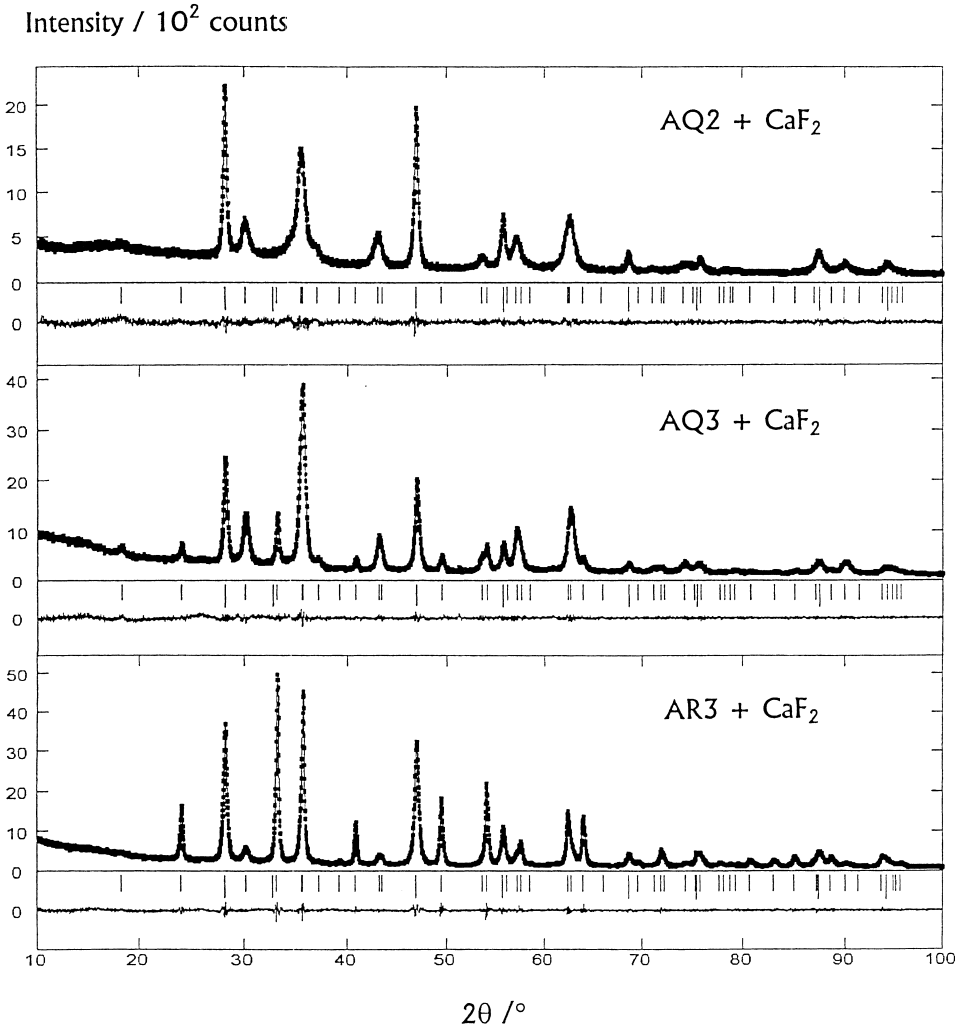

Fig. 5. Whole-powder-pattern decomposition result for samples AQ2, AQ3 and AR3, with CaF_2 as internal standard (Cu K_α data; the split-type pseudo-Voigt profile model and the polynomial background model in calculations). The observed profile intensity is represented by black squares and the calculated intensity by the solid line. Differences between the two intensities are plotted at the bottom of the diagrams on the same scale. Vertical bars are the reflection position markers, longer ones for the reflections of CaF_2.

nents can be ascribed to substoichiometric magnetite ($Fe_{3-x}O_4$), whereas the central quadrupole doublet (1/2eqQ = 0.8 mm s^{-1}) is due to a noncrystallized amorphous, iron(III)-(hydrous) oxide fraction. In this Mössbauer analysis a small fraction of hematite as found with XRD (Table 2) was not taken into account. The spectrum of the AQ3 sample was analyzed with two sites for magnetite, one site for hematite and one site for the amorphous background (smeared subspectrum). The AQ3 sample showed an additional increase in the relative intensity of the outer sextet of the magnetite fraction and this means a further increase in substoichiometry of

Table 3
Refined unit-cell parameter *a* (at room temperature) for magnetite in selected samples

Sample	R_p	R_{wp}	*a* (Å)	Reference
AQ2	0.053	0.068	8.3827(7)	This work
AQ3	0.045	0.060	8.3712(3)	This work
AR2	0.046	0.059	8.3811(5)	This work
AR3	0.048	0.063	8.3593(6)	This work
AR4	0.052	0.069	8.3467(5)	This work
Fe_3O_4			8.3941(7)	[2]
			8.394(5)	[4]
			8.3967	[16], card 19-629

Table 4
Crystallite sizes of magnetite and hematite in samples

Sample	$D_{Fe_3O_4}$ (nm)	$D_{\alpha\text{-}Fe_2O_3}$ (nm)
AQ2	10 (1)	–
AQ3	15 (1)	25 (2)
AR2	11 (1)	20 (2)
AR3	14 (1)	36 (3)
AR4	21 (2)	39 (3)

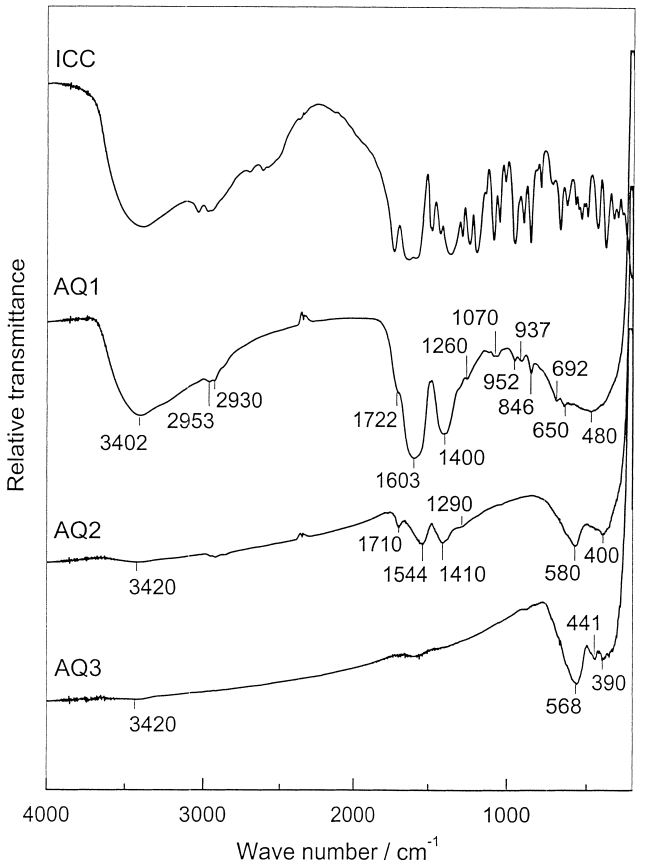

Fig. 6. Fourier transform IR spectra of iron choline citrate and samples AQ1, AQ2 and AQ3, recorded at RT.

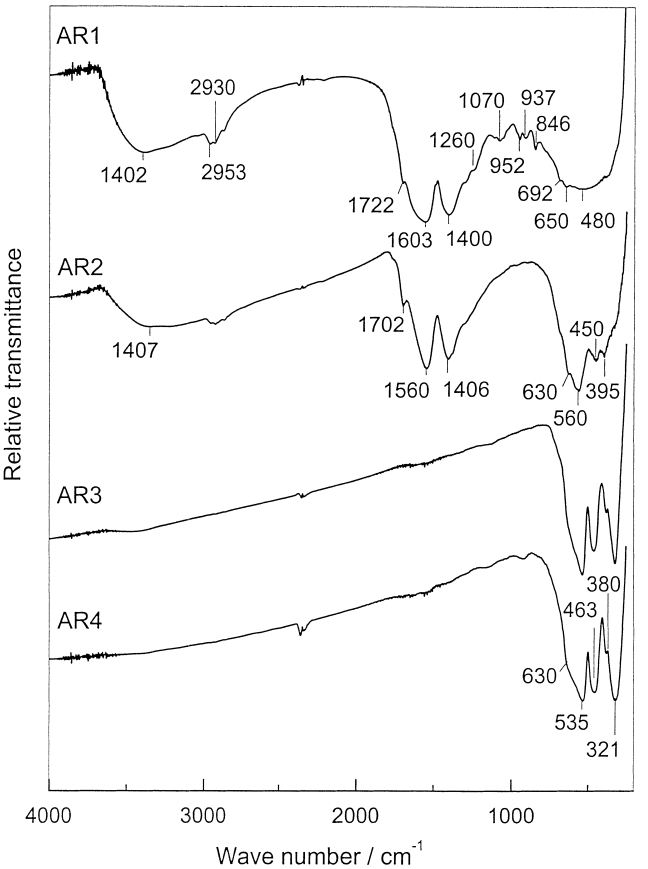

Fig. 7. Fourier transform IR spectra of samples AR1, AR2, AR3 and AR4, recorded at RT.

magnetite, in accordance with the previous discussion on XRD measurements. The ^{57}Fe Mössbauer parameters calculated for samples AQ2 and AQ3 are given in Table 5. On the basis of both, the intensities ratio for magnetite fraction and spectral features shown in Fig. 9, it is evident that the substoichiometric magnetite was formed by thermal decomposition of iron choline citrate. However, in the present case the intensities ratio cannot be taken in formalistic way for calculation of magnetite substoichiometry because the spectra are also affected with the degree of crystallinity and particle size, as well as with high amorphous fraction. The results of Mössbauer phase analysis are in agreement with the phase composition of these samples as determined by XRD (Table 2). Fig. 10 shows the RT Mössbauer spectra of sample AR4 and the hematite standard for comparison. For the AR4 sample the following parameters were calculated: IS = 0.36 mm s^{-1}, 1/2eqQ = −0.18 mm s^{-1}, HMF = 512 kOe and Γ = 0.5 mm s^{-1}. From these data it is clear that the HMF value was slightly reduced in relation to that of hematite (HMF = 517 kOe). Also, the line-width (Γ = 0.5 mm s^{-1}) is increased. A superposition of additional hyperfine magnetic splitting components with the hematite component in this spectrum can be presumed; however, in this

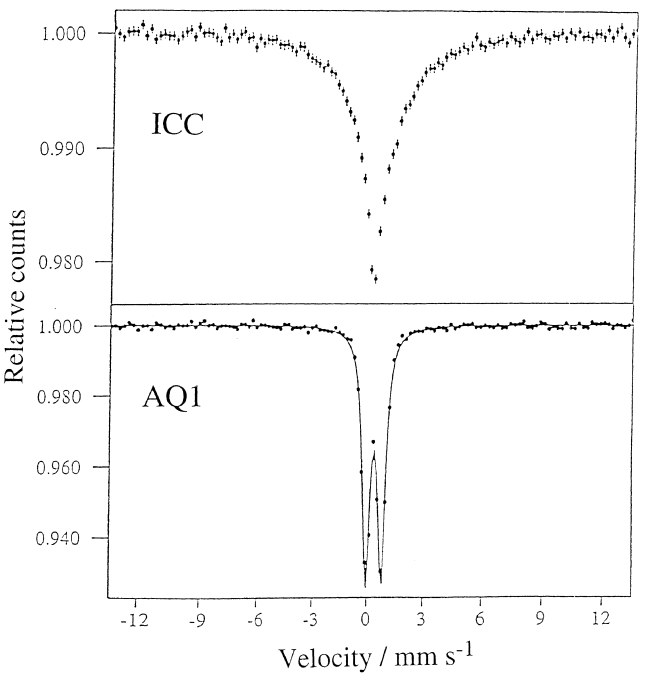

Fig. 8. ^{57}Fe Mössbauer spectra of choline citrate ($C_{33}H_{57}Fe_2N_3O_{24}$) and sample AQ1, recorded at RT.

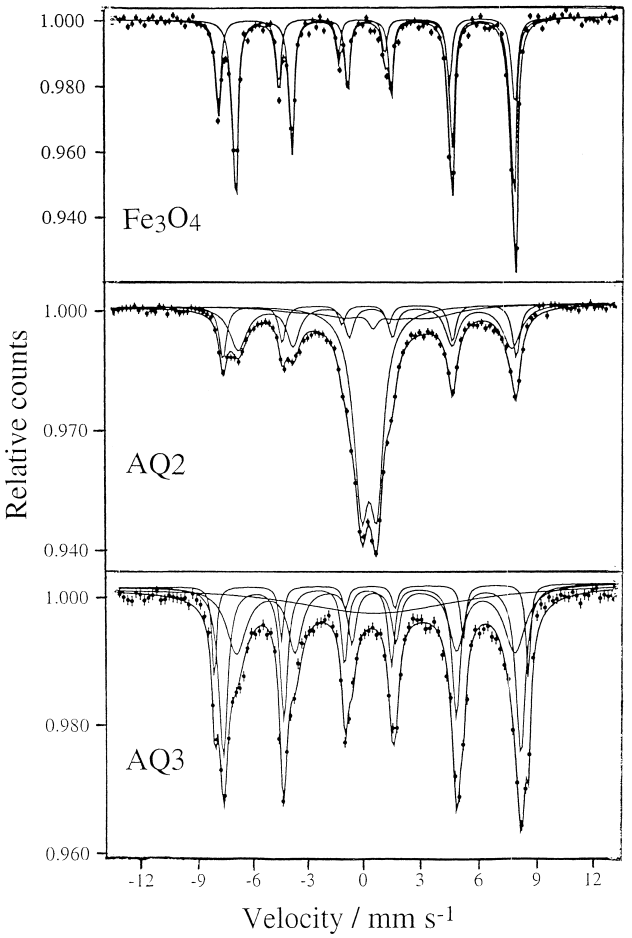

Fig. 9. ^{57}Fe Mössbauer spectra of samples AQ2 and AQ3, and the standard Fe_3O_4. The spectra were recorded at RT.

case there would be a strong overlap between these two spectral components due to similar parameters and they could not be distinquished in physical terms with certainty.

Table 5
^{57}Fe Mössbauer parameters at RT, calculated for samples AQ2 and AQ3

Sample	Component	Intensity (%)	IS[a] (mm s^{-1})	HMF (kOe)	1/4eqQ (mm s^{-1})
AQ2	Fe_3O_4	14	0.34	485	~0
	Fe_3O_4	27	0.57	452	−0.05
	Amorphous	45			0.4
	Amorphous[b]	14	0.5		
AQ3	Fe_3O_4	35	0.30	491	~0
	Fe_3O_4	30	0.57	459	−0.05
	α-Fe_2O_3	10	0.34	518	−0.08
	Amorphous[b]	25	0.5		

Errors: δ and IS = ±0.01 mm s^{-1}. HMF = ±2 kOe.
[a] IS is given relative to α-Fe.
[b] Smeared subspectrum.

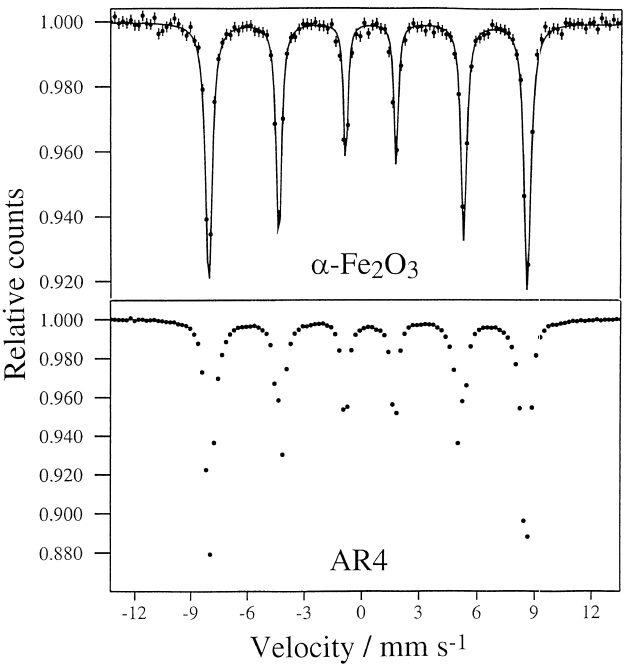

Fig. 10. ^{57}Fe Mössbauer spectra of sample AR4 and the standard α-Fe_2O_3. The spectra were recorded at RT.

4. Conclusions

Thermal decomposition of iron choline citrate has been shown to be a feasible procedure for preparation of nanocrystalline magnetite. The phase composition of the samples depends on the temperature and specifically on the cooling mode. Self-propagating burning of iron choline citrate was observed during the thermal decomposition experiments in air.

Magnetite as a dominant crystalline phase was found in the samples quenched in bidistilled water, whereas in the samples heated at temperatures $T \geq 325$°C and cooled in air the dominant phase was hematite. The amorphous fraction in the samples rapidly decreased with an increase in the temperature of thermal treatment. Also, the unit-cell parameter of magnetite decreased gradually with the increase in temperature of thermal treatment, indicating the substoichiometry of this phase. The crystallite size of magnetite increased from 10(1) to 21(2) nm with increase in the thermal treatment temperature in the range 350–460°C, whereas an increase in the crystallite size of hematite from 25(2) to 39(3) nm was observed.

The FT–IR spectra of the samples quenched in bidistilled water showed a significant fraction of the organic phase, which as a reducing agent favored the formation of magnetite. In the absence, or with traces, of the organic phase a transformation of magnetite into hematite occurs. Self-propagating burning of iron choline citrate favors the formation of hematite as a decomposition product.

The RT Mössbauer spectrum of iron choline citrate showed a single line with pronounced broadening which could be ascribed to a relaxation-type spectrum. On heating at 270°C and quenching in bidistilled water, the sample showed a quadrupole doublet which could be ascribed to an amorphous iron(III)-(hydrous) oxide. For the samples thermally treated at temperatures above 300°C the presence of magnetite and hematite was established. In accordance with the Mössbauer spectra the produced magnetite was substoichiometric, $Fe_{3-x}O_4$, and this substoichiometry significantly increased with the temperature of thermal treatment of the samples, which is in line with the X-ray diffraction studies.

Acknowledgements

The authors wish to thank Professor Stanko Popović of the Department of Physics, Faculty of Science, University of Zagreb, for his valuable discussions.

References

[1] E.J.W. Verwey, J.H. De Boer, Recl. Trav. Chim. Pays-Bas. 55 (1936) 531.
[2] M.E. Fleet, Acta Cryst. B37 (1981) 917.
[3] M.E. Fleet, J. Solid State Chem. 62 (1986) 75.
[4] S. Musić, S. Popović, J. Radioanal. Nucl. Chem. 111 (1987) 27.
[5] R.S. Hargrove, W. Kündig, Solid State Commun. 8 (1970) 303.
[6] G. Galeczki, A.A. Hirsch, J. Magn. Magn. Mater. 7 (1978) 230.
[7] S. Umemura, S. Iida, J. Phys. Soc. Jpn. 47 (1979) 45.
[8] C.M. Srivastava, S.N. Shringi, M.V. Babu, Phys. Stat. Sol. (a) 65 (1981) 731.
[9] S.J. Harker, R.J. Pollard, Nucl. Instrum. Methods Phys. Res. B76 (1993) 61.
[10] P.P. De Abreu Filho, E.A. Pinheiro, F. Galembeck, L.C. Labaki, React. Solids 3 (1987) 241.
[11] Z.X. Tang, S. Nafis, C.M. Sorensen, G.C. Hadjipanayis, K.J. Klabunde, J. Magn. Magn. Mater. 80 (1989) 285.
[12] S.J. Campbell, W.A. Kaczmarek, G.-M. Wang, Nanostructured Mater. 6 (1995) 735.
[13] H. Muramatsu, H. Ito, H. Seharada, S. Shimizu, K. Urushido, T. Miura, Hyp. Int. 84 (1994) 539.
[14] K. Tanaka, T. Yoko, M. Atarashi, K. Kamiya, J. Mater. Sci. Lett. 8 (1989) 83.
[15] T. Fujii, M. Takano, R. Katano, Y. Bando, Y. Isozumi, J. Cryst. Growth 99 (1990) 606.
[16] JCPDS Powder Diffraction File, International Centre for Diffraction Data, Newtown Square, PA 19073-3273, USA.
[17] H.P. Klug, L.E. Alexander, in: X-ray Diffraction Procedures for Polycrystalline and Amorphous Materials, 2nd Edition, John Wiley & Sons, New York, 1974, p. 536.
[18] H. Toraya, J. Appl. Cryst. 19 (1986) 440.
[19] H. Toraya, J. Appl. Cryst. 26 (1993) 583.
[20] L. Alexander, J. Appl. Phys. 25 (1954) 155.
[21] J.E. Iglesias, C.J. Serna, Miner. Petrogr. Acta 29A (1985) 363.
[22] J.E. Iglesias, M. Ocaña, C.J. Serna, Appl. Spectr. 44 (1990) 418.
[23] E. Murad, J.H. Johnston, Iron oxides and oxyhydroxides, in: G.J. Long (Ed.), Mössbauer Spectroscopy Applied to Inorganic Chemistry, Vol. 2, Plenum Publishing Corp, 1987, pp. 507–582.